

# A COMPREHENSIVE METHOD FOR CONCURRENT RECOVERY OF CELLULOSE, NANOCELLULOSE AND LIGNIN FROM DURIAN PEEL: A SUSTAINABLE APPROACH

TRAN Y. DOAN TRANG,\* PHAN THI THUY,\*\* HA THI DZUNG,\*\* TA THI HUONG,\*  
VU DINH GIAP\* and VU THI CUONG\*

\*HaUI Institute of Technology (HIT), Hanoi University of Industry, Hanoi, 11965, Vietnam

\*\*Faculty of Chemical Technology, Hanoi University of Industry, Hanoi, 10000 Vietnam

✉ Corresponding author: T. Y. D. Trang, tydtrang@gmail.com, tydtrang@hau.edu.vn

Received June 19, 2024

Recovering valuable components from agricultural waste is an emerging focus in sustainable development. This study investigates using durian peel (DP) as a raw material for extracting cellulose, nanocellulose (NC), and lignin. The process involves four key stages: (1) pre-treatment, (2) cellulose extraction using 15% (w/v) sodium hydroxide at 100 °C for 2 hours with a ratio of 20/1 mL/g, followed by bleaching with 15% (w/v) hydrogen peroxide overnight, (3) lignin recovery by acidifying the black liquor to pH 1 with concentrated sulfuric acid, and (4) NC extraction through hydrolysis in 64% (v/v) sulfuric acid at 45 °C for 3 hours with a ratio of 20/1 mL/g, followed by neutralization, grinding, centrifugation, filtration, and ultrasonication. The recovery yields were 11.92% for lignin, 54.33% for crude cellulose, 36.03% for pure cellulose, and 29.18% for NC. The NC obtained, characterized as cellulose nanofibrils (CNF), had an average diameter of 114 nm, with 62.23% of particles below 100 nm and 100% below 200 nm. The crystallinity indices were 32.29% for NC and 40.08% for cellulose, while lignin exhibited an amorphous structure. Thermal analysis (TGA) revealed that cellulose degrades more than nanocellulose, indicating that nanocellulose has higher thermal stability. Lignin exhibits excellent thermal stability up to 600 °C, making it suitable for high-temperature applications. These results underscore the potential of DP as a source of valuable bioproducts, including lignin, cellulose, and NC, for diverse industrial applications.

**Keywords:** nanocellulose, lignin, cellulose, durian peel, agricultural waste

## INTRODUCTION

Agriculture is an essential part of the economy and plays a significant role in meeting the needs of society. As the global population continues to rise, it is crucial to improve agricultural productivity. The agricultural sector is projected to provide approximately 24 million tons of food globally to meet the ever-increasing demands of the population.<sup>1</sup> It is worth noting that many agricultural activities concurrently generate significant amounts of waste. This issue impacts the environment and risks human health through environmental pollution, threatening economic stability. Unfortunately, many developing countries lack understanding and efficient implementation of agricultural waste management. This is due to a need for more knowledge about potential risks and benefits. Therefore, sustainable agricultural waste

management methods, such as recycling, recovering valuable components, and implementing green measures are gaining significant attention. These methods reduce emissions and environmental pollution and create opportunities to develop green industries, generate employment, and contribute to efforts toward transitioning to a sustainable ecosystem.<sup>2,3</sup>

Durian (*Durio zibethinus*) is a fruit with a distinctive flavor, often referred to as the “king of fruits”. The largest durian-producing regions in the world are primarily located in Southeast Asia, including Malaysia, Thailand, Indonesia, and Vietnam.<sup>3</sup> Due to its unique flavor and high economic value, durian cultivation has expanded to other tropical regions, such as Australia (Oceania), Madagascar (Africa), Costa Rica, Mexico, and Hawaii (Americas). The rapid

increase in global demand for durian has led various countries to explore expanding their production. According to the Malaysian Ministry of Agriculture and Agro-based Industry (MAFI), the durian industry is experiencing significant growth, with output in Malaysia reaching 390,640 tons in 2020 and projected to reach 443,000 tons by 2030.<sup>4</sup> Similarly, the durian industry in Indonesia has shown significant growth, with yields reaching approximately 10 tons per hectare, and is expected to continue rising in the next decade. However, only 22-30% of the durian fruit is consumed as food, while the rest becomes waste.<sup>3,4</sup> As durian production increases, large amounts of organic waste, mainly from durian peels, are generated. For every 10 million tons of durian produced annually, around 6-7 million tons of organic waste is generated.<sup>5</sup> This waste volume is 2-3 times higher than that of pomelo peels (1.5-2.5 million tons)<sup>6</sup> and equivalent to 28-41% of the waste generated from apples (17-21 million tons per year),<sup>7</sup> and 24-35% of mango waste (15-25 million tons annually).<sup>8</sup> The large-scale durian production and subsequent waste generation have raised environmental concerns, especially when waste management practices, such as burning or landfilling, are improperly conducted.<sup>9,10</sup> The accumulation of durian peel waste poses significant challenges in durian-growing regions, emphasizing the need for sustainable waste management practices. Due to the complex structure of durian husk fibers, their biological decomposition becomes more challenging compared to other lignocellulosic biomass.<sup>11</sup> Various methods have been used to transform this by-product into valuable products, such as durian husk powder, antibacterial membranes, fertilizers, or biochar production.<sup>12,13</sup> Additionally, durian husks have great potential for producing renewable energy, such as bioethanol and biodiesel, given their composition containing cellulose (57.64-60.45%), hemicelluloses (13.09-15.22%), and lignin (15.45-18.45%).<sup>14,15</sup> Meanwhile, durian husks, with components such as cellulose, pectin, lignin, polyphenols, and flavonoids, can also be used as a source of renewable raw materials, addressing waste issues and exploiting valuable components.<sup>16</sup>

Cellulose, a widely abundant biopolymer in biomass, is a crucial material with diverse structures, including both amorphous and crystalline forms.<sup>17</sup> It consists of glucan chains linked by  $\beta$ -1,4-glycosidic bonds, forming a robust and versatile substance.<sup>18</sup> Extracting

natural cellulose fibers from biomass waste and their subsequent chemical transformations can yield various cellulose derivatives.<sup>19</sup> Cellulose is prized for its lightweight, recyclability, biodegradability, and uniform chemical structure, which endows it with exceptional properties, such as high strength, durability, and thermal stability.<sup>17,20</sup> These characteristics make cellulose valuable in numerous industries, including paper, packaging, food, pharmaceuticals, and biofuels.<sup>21</sup> In particular, cellulose derivatives find extensive applications. In the paper industry, cellulose produces various types of paper and cardboard. In the textile industry, it is a critical component of fabrics like rayon and lyocell.<sup>22,23</sup> Additionally, cellulose is employed in producing cellulose acetate for photographic film and in creating biodegradable plastics.<sup>24-26</sup> In pharmaceuticals, cellulose is used as an excipient in tablets and capsules, and in the food industry, it serves as a thickener and stabilizer.<sup>27</sup> Cellulose films, derived from cellulose fibers, also represent an early form of transparent packaging used for products such as snacks, biscuits, and adhesive tapes.<sup>19,28</sup> By understanding and harnessing these properties, cellulose production can address various needs across different sectors.

Building on the unique properties and widespread applications of cellulose, advancements in nanotechnology have led to the development of nanocellulose, a material offering enhanced functionalities and an expanded range of applications. Nanocellulose has gained popularity due to its abundance, low cost, renewability, and significant commercial potential.<sup>29</sup> Its unique physical properties, including low density, porous structure, high biocompatibility, biodegradability, tunable surface chemistry, and superior mechanical strength, make it highly versatile.<sup>29</sup> Moreover, nanocellulose's abundant surface hydroxyl groups, large specific surface area, and chemical reactivity make it an ideal natural nano-building block for various advanced materials.<sup>30-35</sup> Nanocellulose is well-suited for food packaging and pharmaceutical applications thanks to its excellent barrier properties, optical transparency, low thermal expansion, and gas impermeability. It is used in drug delivery systems, green plastics, anti-counterfeiting technologies, and particle tracking.<sup>36</sup> In the biomedical field, nanocellulose has potential in wound healing, tissue engineering scaffolds, and biosensors, as well as in advanced applications like controlled drug release systems

and artificial organs, due to its biocompatibility and ability to incorporate bioactive compounds.<sup>37</sup> In electronics, nanocellulose's flexibility and transparency make it a promising material for flexible displays, sensors, and conductive films.<sup>39</sup> Additionally, nanocellulose is being explored for environmental applications, such as water filtration systems and pollutant absorption, owing to its high surface area and reactivity.<sup>40</sup> In the construction industry, it is incorporated into cement and concrete to improve mechanical properties and reduce material weight, contributing to more sustainable building practices. In energy storage technologies, nanocellulose is used in supercapacitors and batteries, where its mechanical strength and conductivity offer distinct advantages.<sup>41</sup> It is also widely employed as a natural filler in synthetic materials, and its use in developing lightweight, high-strength composites for automotive and aerospace industries highlights its superior mechanical properties and environmental sustainability.<sup>42</sup> With the growing demand for nanocellulose across various industries, continued exploration of new production sources is essential to meet the increasing requirements for this promising material.

Lignin is a significant component of plant cells surrounding cellulose fibers and has the second-highest content after cellulose. Interestingly, the durian rind also contains a considerable amount of lignin, ranging from 10-15%. Unfortunately, lignin is discarded into black liquor and discharged into the environment during cellulose extraction, leading to complex wastewater treatment issues. Moreover, the lignin content in durian peel is also wasted in the environment. Meanwhile, lignin can be used in various industries such as energy, herbicides, rubber processing, iron removal from wastewater, and as a water-softening agent in cationic filter devices.<sup>43</sup> Recent studies show that lignin is highly porous and can treat wastewater containing heavy metals, organic pollutants, and dyes.<sup>44,45</sup> Therefore, recovering lignin has become an urgent issue that needs attention.

However, there has yet to be much research on sustainable agricultural development using durian peel. Most studies focus on recovering individual valuable components, such as polyphenols, pectin, lignin, and cellulose. Researchers from Malaysia have extracted cellulose from durian peel using an acidic sodium chlorite delignification process, followed by alkalization

with 17.5% (w/v) sodium hydroxide. The obtained cellulose has a diameter of about 100-150  $\mu\text{m}$  and is used as a reinforcement material in composite materials.<sup>46</sup> Durian peel is also a potential source of dietary fiber, with the total dietary fiber content being 79.18 g/100 g dry weight, including insoluble dietary fiber – 65.13 g/100 g dry weight and soluble dietary fiber – 13.05 g/100 g dry weight, pectin – 4.11 g/100 g dry weight, hemicelluloses – 18.51 g/100 g dry weight, cellulose – 38.05 g/100 g dry weight, lignin – 2.36 g/100 g dry weight.<sup>47</sup> Researchers Xi Cui and colleagues from Nanyang Technological University in Singapore have transformed durian peel into an antibacterial gel-like bandage.<sup>48</sup> The cellulose powder was extracted from durian peel through air-drying, mixed with glycerol to form a soft gel, and then treated the gel pieces with compounds from baking yeast with antibacterial properties. These bandages keep the injured area cool and moist, aiding wound healing. Nanocellulose fibers obtained from durian peel have been used to reinforce and improve the mechanical properties of concrete. The nanocellulose fibers from durian peel have sizes ranging between 190-255 nm and a width of 22.96 nm. Moreover, composite membranes made by mixing nanocellulose from durian peel with starch, polyvinyl alcohol (PVA), and glycerol have opened up a new avenue for biodegradable packaging that can replace traditional packaging synthesized from petroleum-based raw materials.<sup>10</sup> However, studies only focus on recovering one product from this large waste, which leads to a waste of valuable components in the environment. Therefore, there is a need to focus on simultaneously recovering many economically valuable components based on this agricultural waste source.

The main goal of this study is to create a technological process that can simultaneously extract nanocellulose, cellulose, and lignin from durian peel waste. The study also aims to evaluate the efficiency of each stage to determine suitable technological parameters for each product recovery stage. To describe the characteristics of the recovered products, the study employs various techniques, such as optical microscopy analysis, scanning electron microscopy (SEM), Fourier-transform infrared spectroscopy (FTIR), thermogravimetric analysis (TGA), X-ray diffraction (XRD), and particle size analysis.

**EXPERIMENTAL**

**Materials**

The DP was purchased from the local market in Vietnam and cleaned, drained, and cut into small pieces with sizes of approximately 2-4 mm. Then, the raw material was dried at 60 °C until the weight remained constant using the OFA-240-8 dryer (Esco, Singapore). The dried material was ground using an SK-200 grinder with a power of 1400W (Seka, Japan) and sieved through a 250 µm sieve. The samples were then stored in airtight, dry conditions at room temperature. Some chemicals used in the study were supplied by Sigma-Aldrich (India), including sodium hydroxide (purity 99%), hydrogen peroxide (35% solution), sulfuric acid (95-98%), and hydrochloric acid (30%).

**Methods**

*Approximate chemical composition*

The approximate chemical composition of the raw material was determined using the AOAC method.<sup>49</sup> The moisture content was determined by drying it to a constant weight using a DZF-6090AB vacuum dryer (SHKT-China).<sup>50</sup> Protein content was determined using the Kjeldahl method with an automatic nitrogen

distillation apparatus VELD-UDK 159 (VELP-UDK, Italy).<sup>51</sup> The ash content was determined by ashing to white ash at 550 °C using a LE6/11/B150 muffle furnace (Naberthern, Germany).<sup>29</sup> Fat content was analyzed using a Soxhlet extraction system WHM12293 (Daihan, South Korea).<sup>29</sup> The content of lignin and hemicelluloses was analyzed by standard methods, as described by Song *et al.*<sup>52</sup>

In addition, the cellulose content of the material and in the fiber samples after each treatment was determined. The fiber samples were hydrolyzed using cellulase enzyme at a concentration of 4.8 U/g and incubated at 45 °C for 24 hours to ensure complete hydrolysis of cellulose into glucose.<sup>53</sup> After hydrolysis, the reaction was stopped by heating the mixture at 90 °C for 5 minutes to inactivate the enzyme. The glucose content in the hydrolyzed sample was then quantified using the DNS method.<sup>54</sup>

*Isolation of cellulose, nanocellulose, and lignin*

The process for preparing cellulose, nanocellulose, and lignin was divided into three main stages, as follows: (1) alkali treatment, (2) bleaching, and (3) the nanocellulose isolation process (Fig. 1).

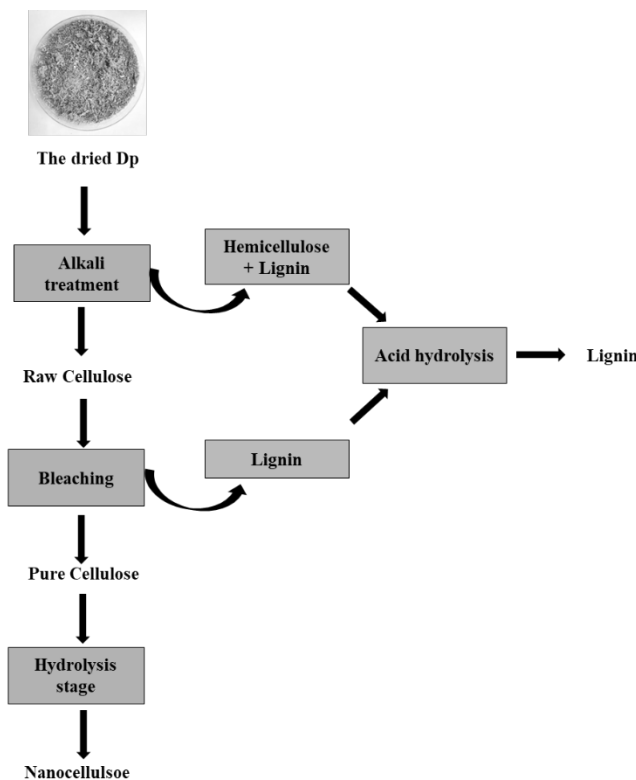


Figure 1: Process for isolating cellulose, nanocellulose, and lignin from DP

*Alkali treatment*

DP powder was treated with a sodium hydroxide solution at a concentration of 10-20% (w/v) and ratios ranging from 1:5 to 1:25 g/mL. The mixture was heated in a Soxhlet extraction system, allowing

continuous extraction and efficient heating at temperatures between 90-120 °C for 1-4 hours. After the alkali treatment, the sample was filtered, and the residue was washed with distilled water until it reached a neutral pH. The residue was then dried to a constant

weight to obtain crude cellulose. The cellulose content in the crude cellulose sample was calculated using formula (1):

$$CC_c = \frac{G_c \cdot 0.9}{m_{cc}} \cdot 100 \quad (1)$$

where  $CC_c$  – the cellulose content in crude cellulose after alkali treatment, %;  $G_c$  – the concentration of glucose in the hydrolysis crude cellulose, g/L; 0.9 – the conversion factor caused by the hydrolysis reaction;  $m_{cc}$  – the mass of crude cellulose after drying, g.

A concentrated sulfuric acid solution was slowly added to the filtrate (also called black liquor) until the pH reached 1. The mixture stood for 24 hours to precipitate the dissolved lignin molecules. The precipitate was then collected and centrifuged at 2000 rpm for 15 minutes. The supernatant was discarded, and the residue was dried to constant weight. The lignin recovery yield after the alkaline treatment stage was calculated using formula (2):

$$H_{l1} = \frac{m_{l1}}{m_{dp}} \cdot 100 \quad (2)$$

where  $H_{l1}$  – the yield of lignin recovery, %;  $m_{l1}$  – the mass of lignin after drying;  $m_{dp}$  – the initial mass of raw material, g.

#### Bleaching

The crude cellulose was bleached using a hydrogen peroxide solution with a concentration ranging from 7.5 to 20% (v/v) for 24 hours, ranging from 1/5 to 1/20 g/mL. After soaking, the mixture was filtered through filter paper and washed with ion-exchange water until a neutral pH was reached. The residue was then dried in an oven at 60 °C until a constant weight was obtained, resulting in pure cellulose. The filtrate was hydrolyzed with concentrated sulfuric acid at pH = 1 for 24 hours. The precipitate was collected from the bottom and centrifuged for 15 minutes at 2000 rpm. The solid obtained was dried until a constant weight was achieved. The cellulose content in the pure cellulose was calculated using formula (3), and the lignin recovery yield during the bleaching stage was calculated using formula (4):

$$CC_b = \frac{G_b \cdot 0.9}{m_{pc}} \cdot 100 \quad (3)$$

$$H_{l2} = \frac{m_{l2}}{m_{cc}} \cdot 100 \quad (4)$$

where  $CC_b$  – the cellulose content in bleached cellulose, %;  $m_{pc}$  – the mass of pure (bleached) cellulose after drying, g;  $G_b$  – glucose concentration in the hydrolysis pure cellulose, g/mL;  $m_{cc}$  – the initial mass of crude cellulose, g;  $H_{l2}$  – the lignin recovery yield in the bleaching, %;  $m_{l2}$  – the mass of lignin in bleaching, g.

#### Nanocellulose (NC) isolation process

Procedure 1: To create nanocellulose, bleached cellulose was mixed with 10% (w/v) hydrogen peroxide and 25% (v/v) sulfuric acid. The mixture was heated to 100 °C for 1 hour with a solution ratio of 20

mL/g. After hydrolysis, a 10% (w/v) dilute solution of hydrogen peroxide and 10% (w/v) sodium hydroxide was added and stirred well with a mechanical stirrer of DH-807 (Osaka®, Japan). The mixture was filtered until it reached a neutral pH and centrifuged at 3000 rpm. After centrifugation, the resultant suspension was subjected to ultrasonication for 10 minutes and stored at 4 °C.<sup>55</sup>

Procedure 2: The acid hydrolysis process of cellulose was conducted according to the description by Mohd Jamil *et al.* with adaptations to suit practical conditions.<sup>29,55</sup> To begin, 25% (v/v) dilute sulfuric acid was added to bleached cellulose at 80 °C for 3 hours. The ratio of sulfuric acid to cellulose was 20/1 mL/g. The hydrolysis process was stopped by adding a solution containing 10% (w/v) hydrogen peroxide and 10% (w/v) sodium hydroxide. The resulting mixture was homogenized using a mechanical stirrer DH-807 (Osaka®, Japan) for 10 minutes. The mixture was centrifuged at 2500 rpm until a neutral pH was reached. The supernatant was then sonicated for 5 minutes to achieve uniform dispersion. Finally, the obtained supernatant was stored at 4 °C.

Procedure 3: Acid hydrolysis with concentrated sulfuric acid was carried out according to the description by Atakhanov *et al.* with modifications.<sup>56</sup> Firstly, cellulose was bleached and hydrolyzed in a 64% (v/v) sulfuric acid solution at 45 °C with a ratio of 20/1 mL/g for 3 hours. After hydrolysis, the mixture was immediately cooled with the tenfold volume of ice water. The mixture was centrifuged at 3000 rpm for 15 minutes. Then, the leaching process was conducted until a neutral pH was reached. The collected portion was centrifuged at 3000 rpm for 10 minutes, and the supernatant was collected for further analysis. The precipitate was sonicated with an ultrasonic bath for 10 minutes.<sup>56</sup>

To evaluate the whole process, the pure cellulose yield ( $H_{tpc}$ ) was calculated according to formula (5), the total lignin yield ( $H_{tl}$ ) was calculated according to formula (6), and the nanocellulose yield ( $H_{nc}$ ) was calculated according to formula (7):

$$H_{tpc} = \frac{m_{pc}}{m_{rm}} \cdot 100 \quad (5)$$

$$H_{tl} = \frac{m_{tl}}{m_{rm}} \cdot 100 \quad (6)$$

$$H_{nc} = \frac{m_{nc}}{m_{rm}} \cdot 100 \quad (7)$$

where  $m_{pc}$  – the mass of pure cellulose obtained, g;  $m_{rm}$  – the initial mass of durian peel powder used, g;  $m_{tl}$  – the mass of lignin obtained throughout the entire process, g;  $m_{nc}$  – the mass of nanocellulose obtained, g.

#### Scanning electron microscopy (SEM)

A scanning electron microscope (Hitachi, Japan) was utilized to describe the morphological characteristics of the samples. The samples were coated onto a small carbon adhesive tape fixed on a copper stub. Afterward, the samples were placed into the SEM chamber, where images of secondary

electron/backscattered dual-angle electrons were captured. The magnification used was 2000 times, and the accelerating voltage of the electron beam was 5000 eV.

#### **Fourier transform infrared spectroscopy (FTIR)**

A Nicolet iS5 FTIR spectrometer (ThermoFisher Scientific, USA) was utilized to describe the chemical composition of the research samples. The infrared spectra of the samples were measured within the wavelength range of 400-4000  $\text{cm}^{-1}$ , with a resolution of 4  $\text{cm}^{-1}$ . The samples were mixed with KBr powder and pressed into thin pellets for analysis.

#### **X-ray diffraction (XRD)**

The relative crystallinity of the research samples was investigated using the X-ray diffraction (XRD) technique with the Ultima IV X-ray diffractometer (Rigaku, USA). The samples underwent scanning across a  $2\theta$  range, employing a step size of  $0.02^\circ$  and a counting time of 0.4 seconds per step. The crystallinity index (CI) of the samples was calculated from the XRD spectra using Equation (8), which involves subtracting the amorphous background:

$$C_I = \frac{I_{200} - I_{am}}{I_{200}} \cdot 100 \quad (8)$$

where  $C_I$ : the crystallinity index, %;  $I_{200}$ : the maximum intensity of the diffraction peak from the (200) plane at  $2\theta = 22.5^\circ$  for cellulose I and  $2\theta = 20.1^\circ$  for cellulose II (crystalline and amorphous regions), and  $I_{am}$ : the intensity value for the amorphous cellulose ( $2\theta = 18^\circ$  for cellulose I and  $2\theta = 16.3^\circ$  for cellulose II (amorphous region)).<sup>57</sup>

#### **Thermal analysis (TGA-DTG)**

The thermal properties of research samples were evaluated using a TGA 209F1 thermal analyzer

(Netzsch, Germany), covering a temperature range of 30-600  $^\circ\text{C}$ . The analysis proceeded with a heating rate of 10  $^\circ\text{C}/\text{minute}$  under nitrogen atmosphere at a 20 mL/minute flow rate.

#### **Particle size analysis**

The particle size of nanocellulose derived from pineapple peel was assessed utilizing a Particle Size Analyzer (PSA) equipped with a Beckman Coulter DelsaTM Nano. After dilution with distilled water and transfer to a cuvette, the PSA device analyzed the sample to ascertain its particle size at room temperature. The measurement span ranged from 10 nm to 4000 nm.

## **RESULTS AND DISCUSSION**

### **Approximate chemical composition**

Various essential components of durian peel powder have been examined and are detailed in Table 1. The findings reveal substantial proportions of cellulose, hemicelluloses and lignin, comprising 37.92%, 10.84%, and 8.48% of the composition, respectively. With such notable composition, durian peel is a promising reservoir for extracting lignin, cellulose, and cellulose derivatives. Notably, the findings regarding durian peel components in this study deviate from prior publications. Thus, the lignin content is lower than that of durian peel sourced from Indonesia, as documented by Masrol S.R. and colleagues (19.3%), while the ash and cellulose contents remain comparable.<sup>58</sup> This variation is attributed to origin, species, geographical location, seasonality, and agricultural practices.<sup>11</sup>

Table 1  
Compositional analysis of DP in this study

Component	Content (%)
Moisture	8.18
Ash	6.57
Cellulose	37.92
Hemicelluloses	8.84
Lignin	10.48

### **Isolation of cellulose and lignin**

Plant lignocellulose fibers consist of three main components: cellulose, hemicelluloses, and lignin, along with pectin, wax, and other compounds. These components form cross-linked structures in plant cells by interacting with hydrophilic hydroxyl groups.<sup>59</sup> To isolate each component, performing reactions that break the bonds between the molecules is necessary.

The alkaline environment provided by sodium hydroxide is considered suitable, economical, and widely used. Sodium hydroxide is a strong base; thus, it can remove hemicelluloses and lignin from crude cellulose.

The crude cellulose obtained after alkaline treatment still contains residual pigments and lignin. Therefore, it must be bleached to remove the remaining components and obtain pure cellulose.

Meanwhile, the filtrate after alkaline treatment and the filtrate after bleaching contain lignin. To recover the dissolved lignin, concentrated sulfuric acid is added to the black liquor to hydrolyze and break the glycosidic and ether bonds between hemicelluloses and lignin. Thus, the lignin precipitates, and can then be quickly recovered through filtration.<sup>60</sup>

#### ***Alkaline treatment process***

The alkaline treatment process separates cellulose from non-cellulosic components, such as lignin, hemicelluloses, wax, *etc.* Lignin is linked to pectin in plant cells through ester bonds between the hydroxyl groups of lignin and the carboxyl groups of uronic acid (a component of pectin chains). Additionally, lignin forms hydrogen bonds with the hydroxyl groups of cellulose, creating a complex spatial network among these components.<sup>59</sup> Agents capable of breaking these cross-links must isolate each component, facilitating the subsequent isolation process.

In an alkaline environment, the bonds between cellulose, hemicelluloses, and lignin are partially broken, separating the cellulose. Under these conditions, lignin molecules are depolymerized into soluble phenolic compounds, while hemicelluloses are hydrolyzed into soluble sugar molecules, thus separating cellulose from hemicelluloses and lignin.<sup>59</sup>

Furthermore, the carboxylic groups of pectin are ionized to form water-soluble sodium carboxylate, which can weaken the intermolecular hydrogen bonds between cellulose chains and other components. The partial removal of lignin, hemicelluloses, pectin, wax, and other extraneous substances from the fiber cell walls during the alkaline treatment makes the cellulose chains more accessible to the agents used in subsequent processing steps, facilitating the production of purer cellulose.<sup>59</sup> Meanwhile, the lignin dissolved in the black liquor can be easily precipitated and recovered using concentrated sulfuric acid. In the alkaline environment, the adhesive lignin molecules contain phenolic groups with weak acidic properties. In such a controlled medium, these lignin molecules carry a negative charge and will bond with sodium ions through reaction. As the pH of the environment decreases, increasing the protonation of phenolic groups and enhanced hydrophobicity of lignin, the lignin molecules precipitate and aggregate together.<sup>61</sup>

The alkaline treatment process effectively recovers both cellulose and lignin. Therefore, this section studies technological factors to maximize the efficiency of obtaining both desired components: crude cellulose and lignin.

#### ***Effect of temperature***

Figure 2 (a) illustrates the relationship between temperature and cellulose content in crude fiber after alkaline treatment and lignin recovery yield from durian peel across a temperature range of 90 °C to 120 °C. The data reveal a clear trend: cellulose content in treated samples and lignin recovery yield rise as the temperature increases. A significant increase is mainly observed between 90 °C and 100 °C. However, further increases beyond 100 °C do not result in statistically significant improvements in either cellulose content or lignin recovery yield ( $p > 0.05$ ).

These findings are consistent with previous studies, which showed that higher temperatures accelerate the breakdown of lignocellulosic structures by weakening hydrogen bonds and van der Waals interactions between cellulose and other components like hemicelluloses and lignin. The process becomes most efficient around 100 °C, where the release and enrichment of cellulose in treated fibers, along with more excellent lignin release into the black liquor, are maximized.<sup>60</sup> Similarly, Mohamad *et al.* (2022) identified 100 °C as the optimal temperature for cellulose extraction from banana stems using NaOH and EDTA,<sup>62</sup> although this temperature is lower than that required for cellulose extraction from sugarcane bagasse (120 °C)<sup>63</sup> and tobacco stems (150 °C).<sup>64</sup> These differences in required temperatures may stem from variations in the lignocellulosic structures of these materials, necessitating higher temperatures to break the bonds between cellulose and other components, such as lignin and hemicelluloses.

Increasing the temperature beyond 100 °C does not further enhance component separation, but results in unnecessary energy consumption. Therefore, maintaining a temperature of 100 °C is the most effective for maximizing cellulose and lignin recovery while minimizing resource use. These findings underscore the importance of optimizing temperature to enhance the efficiency of the recovery process, while reducing solvent and energy consumption.

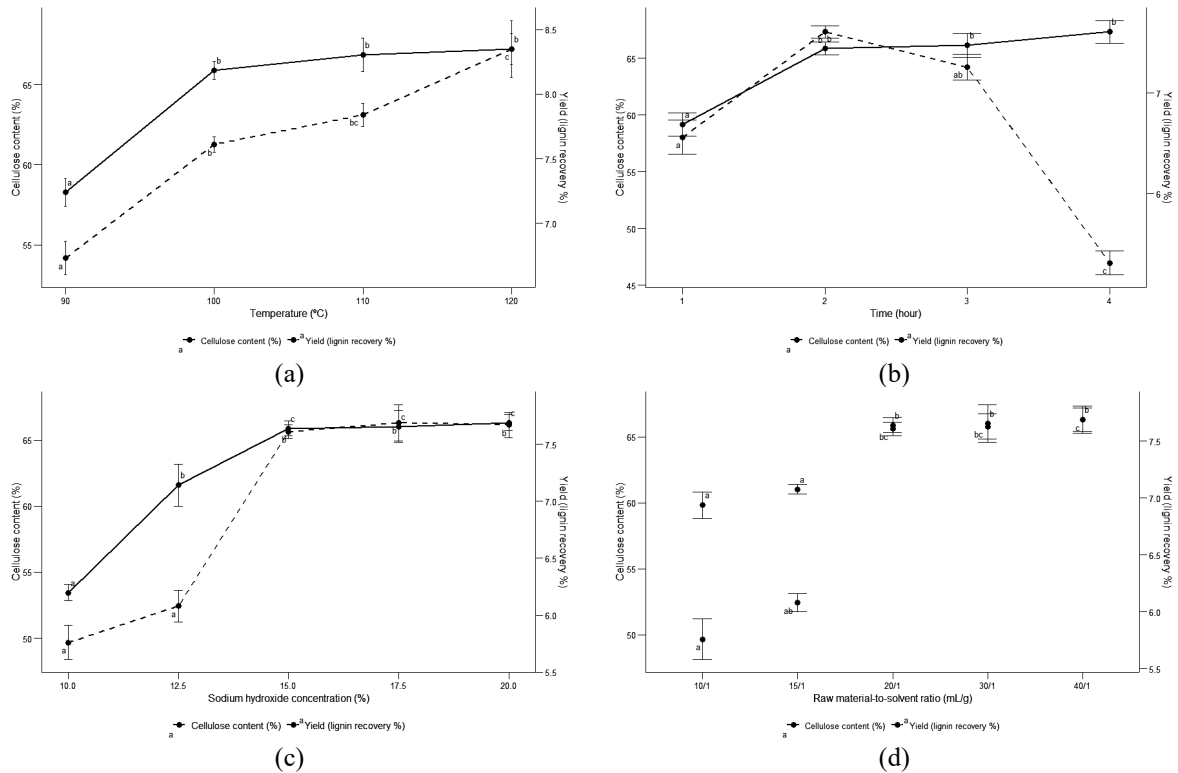


Figure 2: Effect of factors in the alkaline treatment process on the recovery efficiency of crude cellulose and lignin from DP

*Effect of time*

Figure 2 (b) presents the relationship between treatment time and cellulose content in crude fiber after alkaline treatment and lignin recovery yield from durian peel over a duration ranging from 1 to 4 hours. The data show a clear trend: as the treatment time increases, the cellulose content in the treated samples rises, with a particularly significant increase observed between 1 and 2 hours. However, beyond 2 hours, the increase in cellulose content is less pronounced. Statistically, the differences between the 2-hour, 3-hour, and 4-hour treatments are insignificant for cellulose content ( $p > 0.05$ ). In contrast, the yield of lignin recovery increases significantly from 1 hour to 2 hours, but begins to decline after 3 hours. By the 4<sup>th</sup> hour, lignin recovery yield decreases notably, showing a significant reduction compared to the earlier time points. This reduction suggests that prolonged exposure to NaOH might lead to partial degradation of lignin, making it more difficult to recover.

These results align with previous studies on cellulose recovery from banana stems and from olive pomace, which have demonstrated that longer treatment times in alkaline conditions can promote cellulose enrichment by breaking down the bonds between cellulose and hemicelluloses

and lignin, thereby increasing the relative cellulose content in the fiber and the amount of lignin recovered from the black liquor.<sup>62,65</sup> However, extended treatment times may cause lignin to degrade into smaller, more soluble components, reducing the yield of recoverable lignin. Therefore, a treatment time of 2 hours appears optimal for maximizing both cellulose content and lignin recovery. Beyond this point, lignin recovery becomes less efficient, highlighting the importance of optimizing treatment duration to balance cellulose enrichment and lignin yield.

*Effect of sodium hydroxide concentration*

Figure 2 (c) illustrates the effect of sodium hydroxide concentration on the cellulose content of fiber samples after alkaline treatment and the lignin recovery yield from black liquor. The results indicate a clear trend: cellulose content and lignin recovery increase as the sodium hydroxide concentration rises. A particularly significant increase in cellulose content and lignin recovery is observed when the sodium hydroxide concentration increases from 10% to 15%. However, further increases beyond 15% do not statistically significant improvements ( $p > 0.05$ ) in either cellulose content or lignin recovery. This



suggests that higher sodium hydroxide concentrations aid in breaking the bonds between cellulose, hemicelluloses, and lignin, but beyond a certain point, the gains become marginal. Although increasing the sodium hydroxide concentration can enhance the efficiency of lignin recovery and cellulose enrichment, these benefits are limited. Beyond 15%, additional sodium hydroxide does not yield significant improvements, making 15% the optimal concentration for maximizing cellulose and lignin recovery, without unnecessary resource consumption.

In other studies, such as those on banana stems<sup>62</sup> and coir fibers,<sup>66</sup> higher sodium hydroxide concentrations (17.7% and 20%) were required, which is greater than the optimal concentration found in this study. Conversely, lower concentrations were sufficient for cellulose extraction from materials such as sugarcane bagasse (2.75%),<sup>63</sup> tobacco stems (12.5%),<sup>64</sup> and olive pomace (5%).<sup>65</sup> These variations in sodium hydroxide concentration are primarily attributed to differences in the lignocellulosic structure of each material, which dictate the strength of the chemical bonds between cellulose, hemicelluloses, and lignin. Additionally, some extraction methods combine lower sodium hydroxide concentrations with other solvents or use higher temperatures, up to 120 °C, to facilitate the process. This highlights the importance of optimizing extraction conditions to suit the specific characteristics of each raw material and achieve efficient separation of lignocellulosic components.<sup>67</sup>

#### *Effect of raw material-to-solvent ratio*

Figure 2 (d) illustrates the relationship between the solvent-to-material ratio, cellulose content and lignin recovery yield in fiber samples after treatment. The results indicate that increasing the solvent ratio from 10:1 to 20:1 mL significantly enhances both parameters, with further improvements plateauing beyond 20:1 mL. Therefore, a ratio of 20:1 mL/g is optimal for maximizing recovery.

In contrast, the solvent ratio required for extracting cellulose from tobacco stems is considerably lower.<sup>64</sup> This variation is primarily due to differences in the lignocellulosic structures of tobacco stems and durian peel (DP), which result in distinct compositions and arrangements of cellulose, hemicelluloses, and lignin. These structural differences affect the efficiency of the

isolation process. Additionally, the density and porosity of the material influence the solvent's effectiveness. Consequently, adjusting the solvent-to-material ratio based on the specific characteristics of each material is essential for achieving optimal extraction efficiency.<sup>22</sup>

Survey results indicate that the most efficient extraction of crude cellulose and lignin is achieved using a 15% (w/v) sodium hydroxide solution at 100 °C for 2 hours with a material/solvent ratio of 20/1 mL/g.

#### ***Bleaching process***

The bleaching process is a pivotal step in the production of high-quality cellulose. After the initial alkaline treatment, which breaks the bonds between hemicelluloses, lignin, and raw cellulose, the resultant cellulose still contains residual lignin and other coloring compounds. This residual matter renders the cellulose unsuitable for various industrial applications. Therefore, bleaching is essential for removing these remaining contaminants. Oxidizing chemicals, particularly hydrogen peroxide, are commonly used as bleaching agents. During this process, hydrogen peroxide oxidizes and disrupts the bonds between lignin and cellulose, converting these bonds into soluble products that can be removed from the solution. This not only purifies the cellulose, but also enhances its brightness, improving the overall quality of the cellulose, also enabling more efficient recovery of lignin. The soluble products, including lignin and coloring compounds, are subsequently precipitated using concentrated sulfuric acid to isolate the lignin, while the coloring agents are eliminated from the solution.

Different raw materials require specific bleaching conditions due to their varying chemical compositions. For instance, the conditions for bleaching plant peel fibers are generally milder than those for wood fibers, which are often processed at room temperature to reduce heating costs. Thus, key parameters affecting bleaching efficiency for crude fibers derived from durian peels include the concentration of the bleaching agent and the ratio of the bleaching agent to crude cellulose.

#### *Effect of concentration of the bleaching agent*

Figure 3 (a) illustrates the effect of hydrogen peroxide concentration on cellulose content and lignin recovery yield in the samples after bleaching. The data reveal that increasing the

hydrogen peroxide concentration from 7.5% to 12.5% results in a slight increase in cellulose content, with a more significant increase observed from 12.5% to 15% and a plateau at concentrations above 15%. Lignin recovery shows a notable improvement with increased hydrogen peroxide concentration from 7.5% to 10%, a moderate increase from 10% to 15%, and a plateau beyond 15%.

These findings indicate that while higher concentrations of hydrogen peroxide enhance cellulose purity and lignin recovery, concentrations exceeding 15% offer minimal additional benefits and result in unnecessary solvent waste. Therefore, a hydrogen peroxide concentration of 15% is optimal for balancing effectiveness and efficiency in the bleaching process.

*Effect of bleach/crude cellulose ratio*

Figure 3 (b) illustrates the effect of the bleach-to-raw cellulose ratio on the cellulose content in the treated samples and the lignin recovery yield. The results indicate that cellulose content and lignin recovery yield increase significantly as the bleach ratio rises from 10:1 to 15:1 mL/g.

However, increasing the ratio to 20:1 mL/g leads to only marginal improvements in these parameters. This can be explained by the enhanced ability of the bleach to dissolve and remove residual components in the fiber samples, thereby increasing cellulose purity and improving lignin recovery. Nonetheless, at a bleach ratio of 20 mL/g, there is a noticeable reduction in both cellulose content and lignin recovery. This reduction may be related to saturation effects or changes in the dynamics of lignin extraction at excessively high bleach ratios.

These findings suggest that, while increasing the bleach-to-raw cellulose ratio improves cellulose purity and lignin recovery, excessively high ratios offer limited additional benefits and may lead to inefficiencies. Therefore, optimizing the bleach ratio is essential for achieving the best balance between cellulose preservation and lignin recovery efficiency.

Based on the data, the optimal bleaching process parameters are determined as: 15% (w/v) hydrogen peroxide concentration, a bleaching agent to crude cellulose ratio of 15 mL/g, bleaching conducted at room temperature, and overnight soaking.

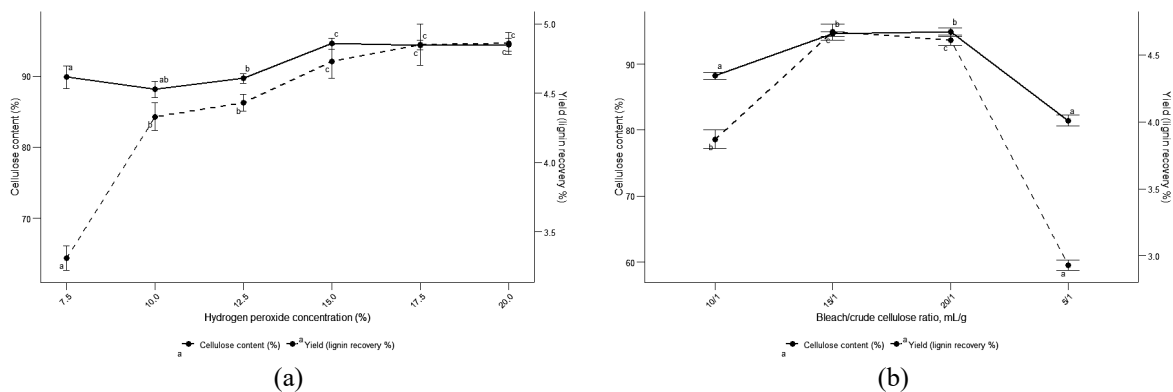


Figure 3: Effects of (a) hydrogen peroxide concentration and (b) bleach/crude cellulose ratio on the cellulose content and lignin yield

**Isolation of nanocellulose**

Various techniques have been developed to process cellulose after bleaching to obtain nanocellulose. The main principle of nanocellulose extraction is to reduce the particle size of cellulose. Different methods have been used, such as mechanical treatment, acid hydrolysis, and enzymatic hydrolysis. Among these methods, acid hydrolysis is particularly effective in reducing cellulose particle size.<sup>56</sup> In this study, three acid-based hydrolysis agents

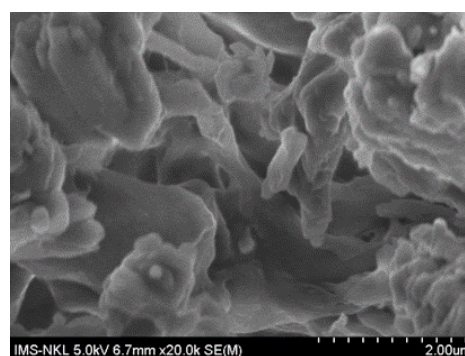
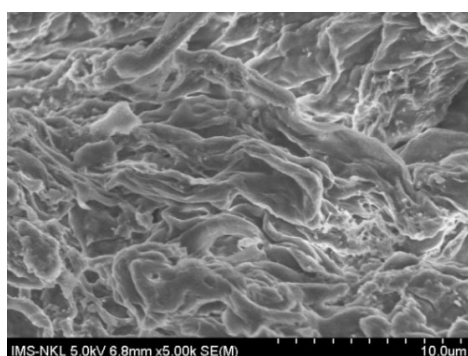
were selected for evaluation. The surface morphology of the nanocellulose samples obtained from these processes was observed using SEM to assess the effectiveness of cellulose chain cleavage by each agent.

The SEM images shown in Figure 4 reveal chain cleavage between cellulose molecules for the nanocellulose samples obtained from a dilute acid environment, both with and without hydrogen peroxide. However, the cellulose fibers remain partially connected, as seen in Figure 4 (a

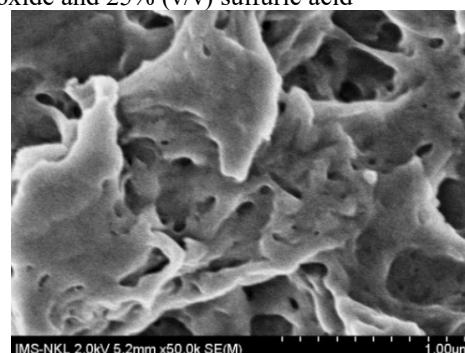
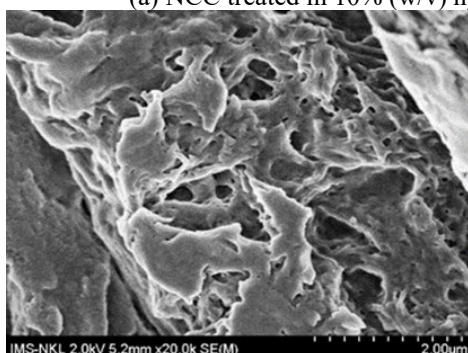
and b). In contrast, the nanocellulose sample hydrolyzed in a concentrated acid environment shows a more significant division of cellulose fibers, resulting in clearly defined smaller particles (Fig. 4 (c)). Nevertheless, the nanocellulose particles tend to aggregate, forming particle chains.

The differences in morphology among the three processes can be explained as follows. In process 3, nanocellulose was obtained under concentrated sulfuric acid conditions, which hydrolyze the strong glycosidic bonds between cellulose units, breaking the cellulose chains into smaller particles.<sup>56,59</sup> For process 1, the

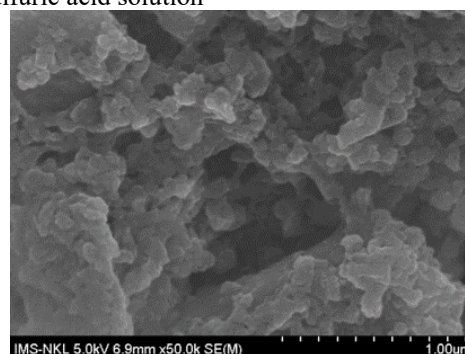
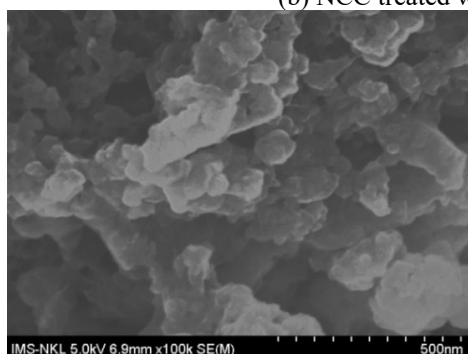
nanocellulose sample was obtained under dilute acid conditions with the addition of hydrogen peroxide. In a sulfuric acid environment, hydrogen peroxide forms OH<sup>-</sup> anions, which attack the hydroxyl groups of cellulose and break the hydrogen bonds between cellulose macromolecules, separating cellulose fibers into smaller sizes.<sup>55</sup> For the sample hydrolyzed in dilute sulfuric acid without hydrogen peroxide, nanocellulose also forms under the influence of sulfuric acid, as evidenced by the fiber cleavage shown in Figure 4 (b). However, the cleavage is incomplete, only partially separating the cellulose fibers.



(a) NCC treated in 10% (w/v) hydrogen peroxide and 25% (v/v) sulfuric acid



(b) NCC treated with dilute sulfuric acid solution



(c) NCC treated with concentrated sulfuric acid

Figure 4: SEM analysis results of NCC samples treated with different processes

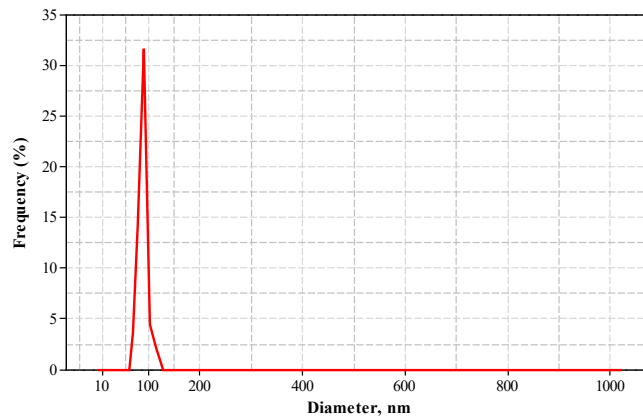


Figure 5: Particle size distribution of nanocellulose derived from DP

SEM data indicate that the concentrated sulfuric acid process is the most effective technique for nanocellulose extraction among the three processes studied.

The particle size analysis was conducted on the nanocellulose samples obtained using the Dynamic Light Scattering (DLS) technique. Figure 5 shows that the nanocellulose particles derived from durian peel have an average diameter of 114.12 nm, with the largest particle size being 145.10 nm and the smallest particle size being 54.65 nm. Approximately 62.234% of the particles have a size smaller than 100 nm, and 100% of the total particles have a size smaller than 200 nm.

#### Proposed process for nanocellulose and lignin extraction from durian peel

The manufacturing process for lignin, cellulose, and nanocellulose, illustrated in Figure 6 (flow chart), is based on thorough research into alkali treatment, bleaching, and cellulose hydrolysis stages. This process consists of four main stages:

- Stage 1: Pretreatment stage – in the initial stage, the raw material undergoes pretreatment, turning it into a fine powder. This step aims to improve storage and preservation while facilitating subsequent processing stages;
- Stage 2: Cellulose recovery stage – this crucial stage involves two primary steps: alkali treatment and bleaching. These processes produce two essential products: raw cellulose and bleached cellulose, vital raw materials for the paper and packaging industries;
- Stage 3: Lignin recovery stage – after alkali treatment, lignin is recovered from the resulting black liquor. Acidification with a

sulfuric acid solution to pH = 1 enables the separation and retrieval of lignin;

- Stage 4: Nanocellulose recovery stage – the final stage focuses on extracting nanocellulose from bleached cellulose. Pure cellulose fibers undergo hydrolysis and cleavage in a concentrated sulfuric acid environment. Mechanical grinding and ultrasonic treatment further aid in size reduction, producing significantly smaller nanocellulose particles.

Lignin, cellulose, and nanocellulose components were isolated according to the proposed process. The efficiency of each product was calculated and recorded in Table 2. After alkali treatment and bleaching, the lignin extraction efficiency was 11.92%. Notably, the lignin content obtained from durian peel powder in this study is higher than that extracted from *Cynara cardunculus* using enzyme methods (8.5-11.7%)<sup>68</sup> and significantly higher than that from wheat straw (2.3-3.5%),<sup>69</sup> and sugarcane bagasse (3.4-3.9%).<sup>70</sup> However, it is lower than the lignin extraction efficiency from spruce wood using hot water extraction (22.5%).<sup>71</sup> The efficiency of crude cellulose and pure cellulose extracted from durian peel was 54.33% and 36.03%, respectively. This suggests that the cellulose content in durian peel is lower than that in wheat straw (59.7-63.5%),<sup>69</sup> and *Miscanthus sinensis* biomass (70.4-78.63%),<sup>72</sup> but higher than cellulose recovered from mixed waste of various fruits and vegetables (8.81-16.13%),<sup>73</sup> and sugarcane bagasse (44.7-45.9%).<sup>70</sup> As for nanocellulose, the efficiency reached 29.18% based on the dry weight of durian peel powder. Therefore, it is evident that durian peel is a potential source of valuable components, such as lignin, cellulose, and nanocellulose. Recovering these valuable components for application in various fields will increase the

utilization of agricultural by-products in general and pineapple peel in particular and also contribute to addressing a significant amount of

solid waste generated by the agricultural sector, which currently occupies large areas of landfills.

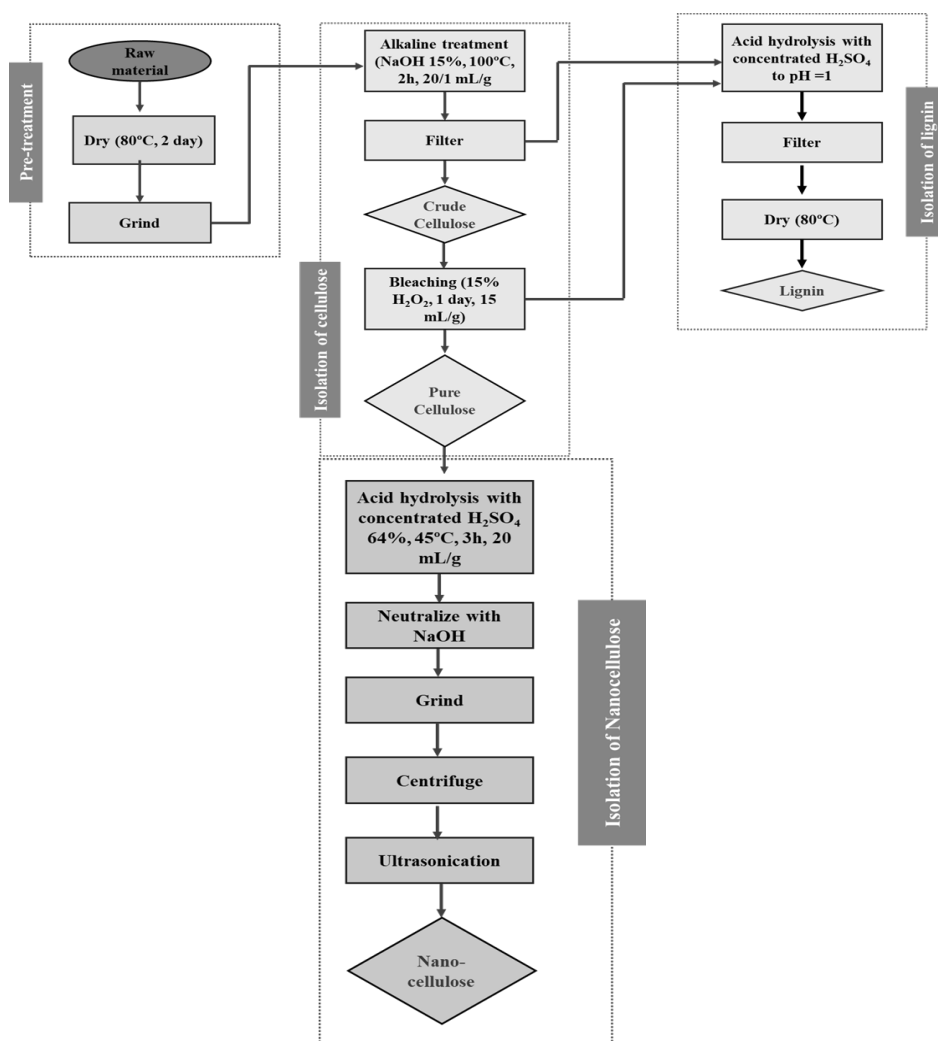
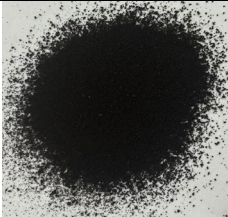



Figure 6: Flow chart of the process for obtaining lignin, cellulose, and nanocellulose from DP

Table 2

Isolation efficiency and visual representation of lignin, cellulose, and nanocellulose components

Component	Yield, %	Visual representation
Lignin	11.92	
Crude cellulose	54.33	

Pure cellulose	36.03	
Nanocellulose	29.18	

### Characterization of lignin, cellulose and nanocellulose from DP

#### FTIR analysis

The FTIR spectrum was used to analyze the functional groups in the products recovered from durian shell powder. The FTIR results of nanocellulose (Fig. 7a) and cellulose (Fig. 7b) obtained from durian peel show that the peaks are almost identical. Specifically, the appearance of peaks at  $3442\text{ cm}^{-1}$  is characteristic of the stretching vibrations of OH stretching. The peak appearing at a wavelength of  $2923\text{ cm}^{-1}$  is related to the C-H bonds present in the structure of the glucopyranosic ring.<sup>74</sup> The absence of peaks in the  $1750\text{--}1700\text{ cm}^{-1}$  region indicates that nanocellulose and cellulose from DP are not in an oxidized form or do not have carboxylic groups.<sup>74</sup> The peak at  $1634\text{ cm}^{-1}$  is attributed to the vibration of hydroxyl groups. Meanwhile, the absorption peak at  $1060\text{ cm}^{-1}$  is assigned to C-O stretching vibrations. However, the OH stretching absorption in nanocellulose is stronger compared to cellulose. This is because when the cellulose molecules are smaller, more free hydroxyl groups are exposed on the surface. In other words, the number of free hydroxyl groups in nanocellulose is higher than in cellulose fibers.<sup>75</sup> Additionally, the absence of new peaks in the FTIR results of nanocellulose indicates that hydrolyzing cellulose into nanocellulose does not form any new bonds, but only serves to cut the cellulose chains into smaller molecules. These results are consistent with the FTIR analysis of cellulose and

nanocellulose obtained from rice straw and poplar wood,<sup>75</sup> pineapple peel,<sup>76</sup> and chili waste.<sup>77</sup>

In the FTIR spectrum of lignin, the peak at  $3348\text{ cm}^{-1}$  is attributed to hydrogen bonding in the  $\text{--OH}$  group. The peak at  $2925\text{ cm}^{-1}$  is primarily assigned to methyl and methylene groups. The C=O stretching vibration of the carboxylic groups in lignin is absorbed at the peak at  $1710\text{ cm}^{-1}$ . Sharp peaks at  $1632\text{ cm}^{-1}$  and  $1429\text{ cm}^{-1}$  indicate the vibrations of the aromatic ring. The peak at  $1044\text{ cm}^{-1}$  signifies aromatic C-H in-plane deformation. These results are consistent with those for lignin recovered from the formic acid process,<sup>78</sup> from eucalyptus wood powder,<sup>79</sup> lignin obtained from various plants,<sup>80</sup> and lignin from Moroccan thuya wood.<sup>81</sup>

#### SEM

The surface morphology of lignin observed under the scanning electron microscope (SEM) (Fig. 8 (a)) reveals the structural morphology of lignin particles. The lignin particles are porous and aggregate into large conglomerates.<sup>11</sup> The surface of the lignin mass, characterized by numerous microscopic pores, appears relatively rough and uneven, increasing the porosity of the lignin. Additionally, the lignin structure from durian peel is observed to consist of small interconnected particles, most of which have compact structures with relatively uniform sizes. Similar observations have been found for lignin extracted from rice husk,<sup>82</sup> Moroccan thuya,<sup>81</sup> acetylated lignin,<sup>83</sup> and industrial lignin.<sup>84</sup>

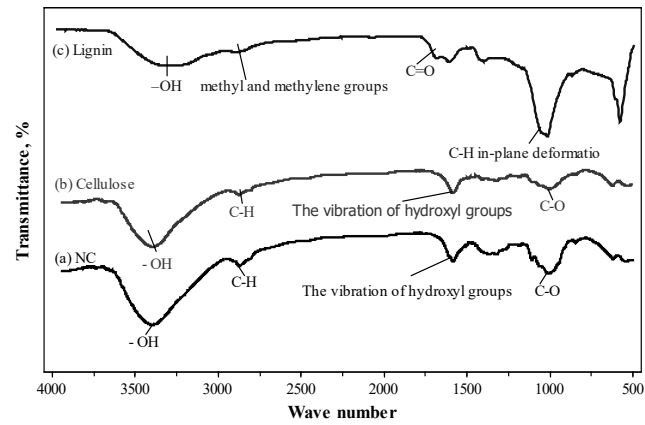


Figure 7: FTIR results of (a) bleached cellulose, (b) nanocellulose; and (c) lignin from DP

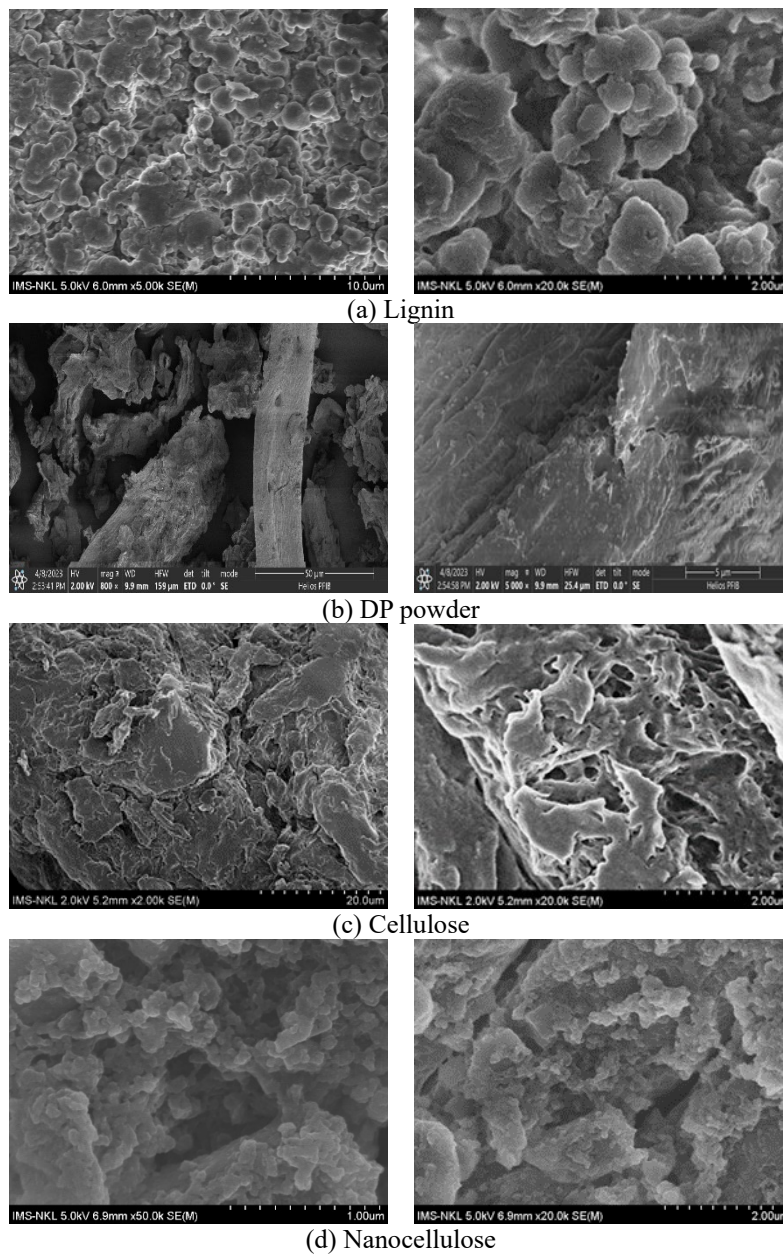


Figure 8: SEM of (a) lignin, (b) DP powder (c) pure cellulose and (d) nanocellulose from DP

The scanning electron microscopy (SEM) analysis of raw durian peel (Fig. 8 (b)) powder reveals a smooth surface structure. This is due to the presence of lignin, cellulose, and hemicellulose components bonded together to form plant cells. Consequently, the surface of the durian peel at this stage appears as fine fibers.<sup>59</sup> Figure 8 (c and d) illustrates the morphology of cellulose and nanocellulose extracted from the durian peel. The obtained cellulose has a rough surface with some surface fragmentation, though the fibers are not entirely separated from each other. This is attributed to removing hemicellulose and lignin components, allowing for more precise separation of the cellulose fibers.<sup>59</sup>

Meanwhile, nanocellulose obtained from durian peel treated with concentrated acid exhibits numerous tiny particles with uniform sizes, resulting in a significantly rougher surface than the cellulose sample (Fig. 8 (b)). The nanocellulose surface also shows a noticeable increase in the fragmentation of cellulose fibers compared to the pure fibers. The structure of nanocellulose derived from durian peel can enhance the reinforcement in other material matrices, improving the properties of the base material through enhanced interaction between components.<sup>85</sup>

#### ***X-ray diffraction analysis (XRD)***

The mechanical and thermal properties of the studied samples are linked to the level of crystallinity. The cellulose, nanocellulose, and lignin isolated from durian rind were examined for crystallinity using X-ray diffraction (XRD) (Fig. 9). The X-ray diffraction patterns of cellulose and nanocellulose derived from durian rind exhibit peaks at 35.1° and 34.7°, ascribed to the amorphous region's diffraction intensity. The most prominent diffraction peaks are observed at 20.2° and 22.2° for cellulose and at 20.4° and 22.5° for nanocellulose on the diffraction patterns of cellulose and nanocellulose, respectively. This suggests that the cellulose and nanocellulose from durian rind in this study possess a mixed structure of cellulose type I and type II, indicating that the structures of both nanocellulose and cellulose blend crystalline and amorphous regions. However, a comparison between the XRD patterns of cellulose and nanocellulose reveals that the diffraction angles decrease after the hydrolysis of cellulose into nanocellulose,

indicating the complete removal of hemicelluloses and other carbohydrates from the cellulose molecule.<sup>86</sup> The crystallinity index of the cellulose sample was found to be approximately 54.74%, while the nanocellulose sample had a crystallinity index of about 39.95%. The reduction in the intensity of the crystalline peaks in the XRD patterns of nanocellulose can be explained by several factors. First, as the size of the crystalline particles decreases, the surface area increases, leading to more substantial surface effects and scattering, reducing the intensity of X-ray diffraction. This effect is commonly observed in nanomaterials like nanocellulose.<sup>87</sup> Second, the acid hydrolysis process can reduce the crystallinity of the material by removing amorphous regions and decreasing the size of crystalline domains, making the structure less ordered and thus lowering the intensity of the crystalline peaks.<sup>88</sup> Additionally, defects in the crystal lattice, such as stacking faults or distortions, can reduce the regularity of the crystalline structure, causing X-ray scattering to become more diffuse.<sup>89</sup> All these factors combined contribute to the reduced intensity of the crystalline peaks in the XRD patterns of nanocellulose. The crystallinity of cellulose from durian rind is lower than that of cellulose extracted from chili stems (50.78%),<sup>77</sup> but comparable to the crystallinity of cellulose extracted from rice straw (30-55%).<sup>90</sup> Meanwhile, the crystallinity of nanocellulose in this study was found to be lower than that of nanocellulose extracted by acid hydrolysis from rice straw (35-45%)<sup>90</sup> and cotton (48-64%)<sup>91</sup> and higher than nanocellulose from okra (*Abelmoschus esculentus*) fiber (29%).<sup>92</sup>

The X-ray diffraction of lignin does not exhibit any peaks, indicating that lignin molecules lack a crystalline structure and instead exist in an amorphous form. This can be attributed to the fact that the lignin was obtained under high-concentration acid conditions, which is known to decrease crystallinity as the acid concentration increases. Several reports have also noted that the diffraction angles of lignin are highly diverse and vary based on the source material and the method of lignin isolation.<sup>86</sup> The X-ray diffraction pattern of lignin from durian rind closely resembles the XRD pattern of industrial lignin<sup>93</sup> and acetylated lignin from oil palm empty fruit bunches.<sup>83</sup>



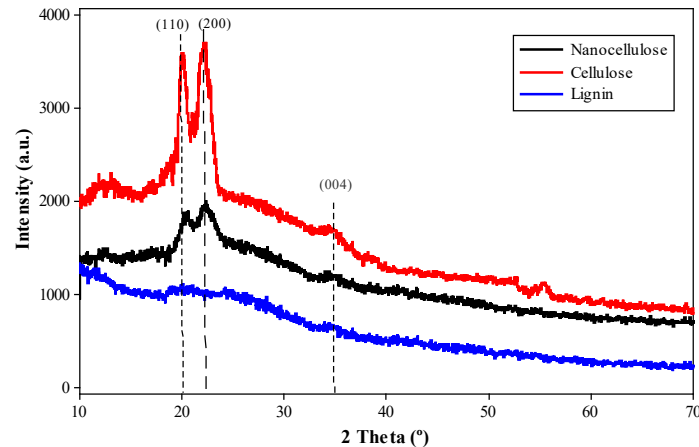


Figure 9: X-ray diffraction patterns of lignin, cellulose, and nanocellulose obtained from DP

### ***Thermogravimetric (TGA) and differential thermogravimetric (DTG) analyses***

Figure 10 illustrates the thermal stability and differential thermogravimetric analysis of cellulose, nanocellulose, and lignin. Both cellulose and nanocellulose exhibit three primary regions of weight loss, although the temperature ranges for these regions differ between the two materials. The first weight loss region, occurring at 60-120 °C for cellulose and 75-100 °C for nanocellulose, is attributed to the evaporation of water present in the materials.<sup>92</sup> Nanocellulose shows a weight loss of approximately 19.74%, compared to 9.31% for cellulose, reflecting the higher moisture content in nanocellulose.<sup>94</sup> Additionally, DTG analysis reveals that the rate of weight loss in nanocellulose is faster than that of cellulose during this stage. The second region involves the decomposition of esterified cellulose chains and hydroxyl groups. For nanocellulose, this occurs at 120-180 °C, while for cellulose, it occurs at 100-120 °C.<sup>95</sup> In this region, nanocellulose experiences a total weight loss of around 11.26%, compared to 4.65% for cellulose. This disparity is likely due to the higher number of hydroxyl groups in nanocellulose after acid hydrolysis. The smaller size of nanocellulose exposes more hydroxyl groups, leading to a faster decomposition rate in nanocellulose (-4.41%/min) compared to cellulose (-2.79%/min). The third weight loss region, occurring between 190-240 °C for nanocellulose and 140-360 °C for cellulose, is attributed to the initial degradation of the cellulose polymer, including depolymerization, dehydration, and breakdown of glycosidic units.<sup>95</sup> Although cellulose begins structural decomposition earlier than nanocellulose, it experiences a significantly faster and more pronounced weight loss in this stage. This is

evident in the TGA and DTG curves (Fig. 10 (a)), where cellulose shows a distinct degradation curve and a prominent third peak. The fourth region, occurring above 350 °C for nanocellulose and above 400 °C for cellulose, is associated with the decomposition of carbon chains. At 600 °C, the weight loss is 62.38% for nanocellulose and 65.96% for cellulose. This difference in thermal stability may be attributed to the hydrolysis process in the sulfuric acid environment, which introduces sulfate groups in nanocellulose. These sulfate groups may create stronger bonds between molecules, enhancing the thermal stability of nanocellulose compared to cellulose.<sup>96</sup> Additionally, the smaller size of nanocellulose further contributes to its improved thermal stability. Overall, cellulose is less thermally stable and more susceptible to severe thermal conditions than nanocellulose in this study.<sup>97</sup> Similar results were also observed for cellulose and nanocellulose derived from *Ulva lactuca*<sup>98</sup> and office wastepaper.<sup>96</sup>

The differential thermal analysis of lignin shows that weight loss occurs insignificantly up to 600 °C. However, three central weight loss regions of lignin are observed. The first region occurs from 60-110 °C, related to the evaporation of water in the extracted lignin.<sup>99</sup> The subsequent slow decomposition in the temperature range of 160-220 °C is attributed to the dehydration of chemically bound water and the hydroxyl groups in lignin,<sup>100</sup> leading to a weight loss of about 1.08%. The third transition region occurs at 240-440 °C, resulting from the partial decomposition of carboxylic and anhydride groups and the residual hemicelluloses in lignin.<sup>100,101</sup> The weight loss at 600 °C is only 5.84%, which is relatively

insignificant. This indicates that the lignin in this study has good thermal stability, making it suitable for applications requiring high thermal

stability or for use in producing lignin-containing charcoal.

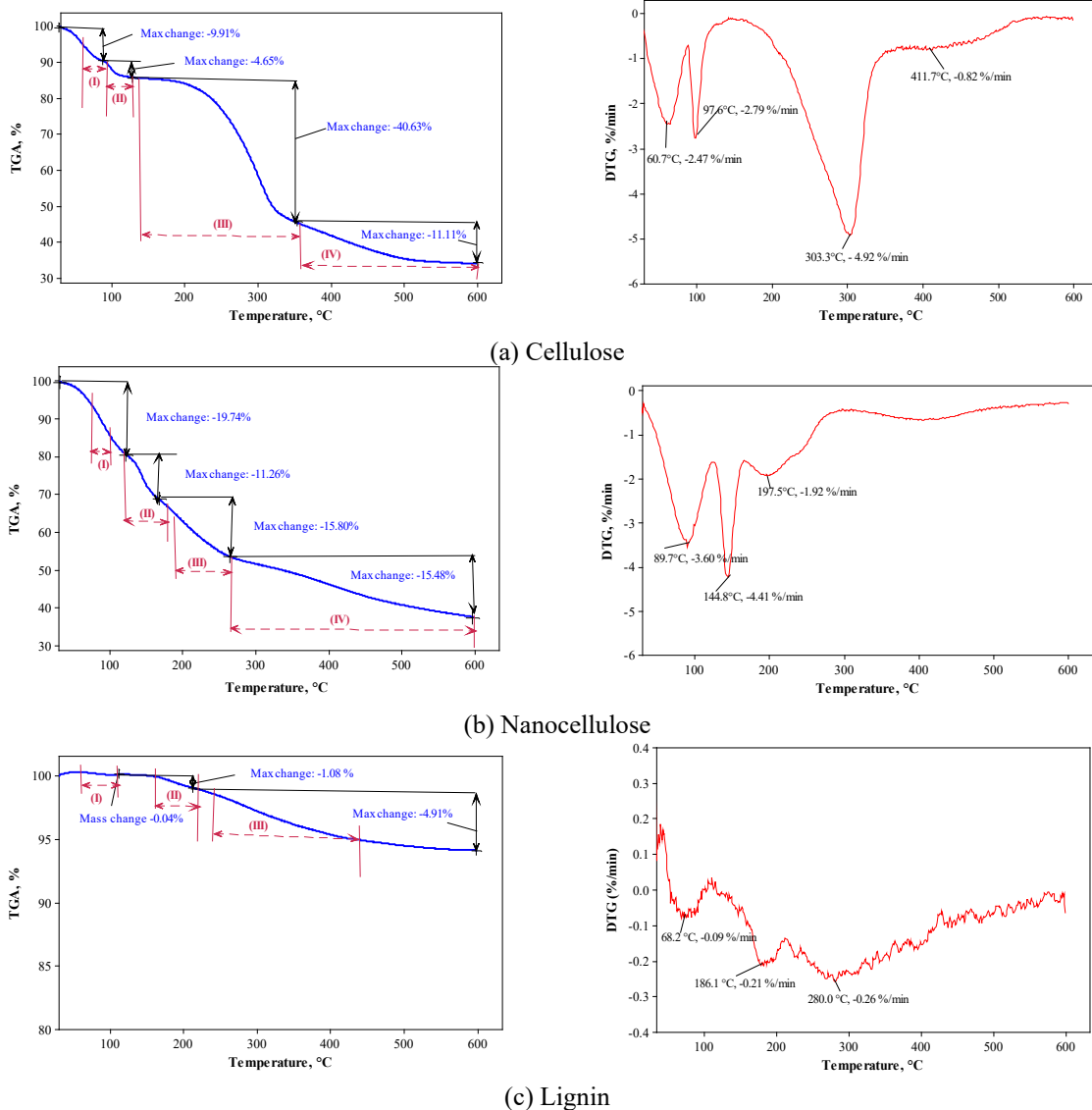


Figure 10: TGA and DTG curves of cellulose, nanocellulose, and lignin-derived from DP

**CONCLUSION**

This study presents a highly efficient and sustainable process for the simultaneous recovery of cellulose, nanocellulose, and lignin from durian peel, demonstrating the potential of agricultural waste as a valuable resource. The process, consisting of pre-treatment, sodium hydroxide treatment, bleaching, and acid hydrolysis, yielded substantial amounts of critical products: 54.33% crude cellulose, 36.03% purified cellulose, 29.18% nanocellulose, and 11.92% lignin. The recovered nanocellulose, classified as cellulose nanofibrils, exhibited a favorable particle size distribution, with 62.23% of particles measuring

below 100 nm and all particles under 200 nm. Crystallinity indices of 32.29% for nanocellulose and 40.08% for cellulose indicate their structural integrity. Furthermore, thermal analysis confirmed the excellent thermal stability of nanocellulose compared to cellulose, while lignin demonstrated remarkable stability up to 600 °C, highlighting its suitability for high-temperature applications. These results underscore the feasibility of utilizing durian peel for the eco-friendly recovery of high-value bioproducts. The developed process offers a scalable solution, contributing to the circular economy by transforming agricultural waste into industrially

relevant materials with potential applications in bioplastics, nanocomposites, and high-temperature industries.

**ACKNOWLEDGMENTS:** The authors would like to thank Hanoi University of Industry for funding this research through project number 38-2023-RD/HĐ-ĐHCN and the HaUI Institute of Technology (HIT) at Hanoi University of Industry for supporting the facilities used to obtain the results of this study.

## REFERENCES

- <sup>1</sup> Food and Agriculture Organization of the United Nations (FAO), 2017
- <sup>2</sup> S. Bracco, O. Calicioglu, M. G. S. Juan and A. Flammini, *Sustainability*, **10**, 1698 (2018), <https://doi.org/10.3390/su10061698>
- <sup>3</sup> N. Scarlat, J. F. Dallemand, F. Monforti-Ferrario and V. Nita, *Environ. Develop.*, **15**, 3 (2015), <https://doi.org/10.1016/j.envdev.2015.03.006>
- <sup>4</sup> T. Y. D. Trang, P. H. Quynh, T. T. Huong, D. T. Hanh, H. T. Dzung *et al.*, *Food Sci. Technol.*, **12**, 128 (2024), <https://doi.org/10.13189/fst.2024.120202>
- <sup>5</sup> R. Bhat and G. Paliyath, "Encyclopedia of Food and Health", 2016, pp. 138-143 <https://doi.org/10.1016/B978-0-12-384947-2.00337-8>
- <sup>6</sup> Food and Agriculture Organization of the United Nations (FAO), 2023
- <sup>7</sup> L. Xiao, F. Ye, Y. Zhou and G. Zhao, *Food Chem.*, **351**, 129247 (2021), <https://doi.org/10.1016/j.foodchem.2021.129247>
- <sup>8</sup> I. Shahzadi, S. Mubarak, A. Farooq and N. Hussain, *Aqua - Water Infrast. Ecosyst. Soc.*, **72**, 914 (2023), <https://doi.org/10.2166/aqua.2023.216>
- <sup>9</sup> S. Marçal and M. Pintado, *Trends Food Sci. Technol.*, **114**, 472 (2021), <https://doi.org/10.1016/j.tifs.2021.06.012>
- <sup>10</sup> S. Rahmawati, Rabasia, Afadil, Suherman, T. Santoso *et al.*, *Jurnal Pengelolaan Sumberdaya Alam dan Lingkungan* [Journal of Natural Resources and Environmental Management], **13**, 76 (2023), <https://doi.org/10.29244/jpsl.13.1.76-87>
- <sup>11</sup> Z. R. F. Romadhon and I. G. Made Sanjaya, *Jurnal Akademika Kimia*, **10**, 230 (2021), <https://doi.org/10.22487/j24775185.2021.v10.i4.pp230-236>
- <sup>12</sup> A. K. Obeng, D. Premjet and S. Premjet, *Peer. J.*, **9**, e12026 (2021), <https://doi.org/10.7717/peerj.12026>
- <sup>13</sup> R. Jiamjariyatam, W. Thongrod and N. Koocharoenpisa, *J. Culin. Sci. Technol.*, **2023**, 1 (2023), <https://doi.org/10.1080/15428052.2023.2199694>
- <sup>14</sup> A. Manmeen, P. Kongjan, A. Palamanit and, R. Jariyaboon, *Biomass Bioenerg.*, **174**, 106816 (2023), <https://doi.org/10.1016/j.biombioe.2023.106816>
- <sup>15</sup> J. Ratanapoompinyo, P. Yasurin, T. Phusantisampan, P. Tantayotai, E.J. Panakkal *et al.*, in *Procs. 2020 Int. Conf. Utility Exhibition on Energy, Environ. and Climate Change (ICUE)*, Pattaya, Thailand, 2020, pp. 1-8, <https://doi.org/10.1109/ICUE49301.2020.9307146>
- <sup>16</sup> E. J. Panakkal, K. Cheenkachorn, M. P. Gundupalli, N. Kitiborwornkul and M. Sriariyanun, *J. Indian Chem. Soc.*, **98**, 100264 (2021), <https://doi.org/10.1016/j.jics.2021.100264>
- <sup>17</sup> P. Rachtanapun, S. Luangkamin, K. Tanprasert and R. Suriyatem, *LWT-Food Sci. Technol.*, **48**, 52 (2012), <https://doi.org/10.1016/j.lwt.2012.02.029>
- <sup>18</sup> C. Trilokesh and K. B. Uppuluri, *Sci. Rep.*, **9**, 16709 (2019), <https://doi.org/10.1038/s41598-019-53412-x>
- <sup>19</sup> H. Wang, H. Xie, H. Du, X. Wang, W. Liu *et al.*, *Carbohydr. Polym.*, **239**, 116233 (2020), <https://doi.org/10.1016/j.carbpol.2020.116233>
- <sup>20</sup> N. W. Y. Vanessa, N. C. Huey, T. Y. Peng, O. Z. Xian and S. S. Hoong, *Cellulose Chem. Technol.*, **55**, 311 (2021), <https://doi.org/10.35812/CelluloseChemTechnol.2021.55.31>
- <sup>21</sup> H. Du, C. Liu, M. Zhang, Q. Kong, B. Li *et al.*, *Prog. Chem.*, **30**, 448 (2018), <https://doi.org/10.7536/PC170830>
- <sup>22</sup> A. Amir, J. Somayeh and A. Nazanin, *Iranian J. Chem. Chem. Eng.*, **43**, 499 (2024)
- <sup>23</sup> R. Nayak, D. Cleveland, G. Tran and F. Joseph, *J. Mater. Sci.*, **59**, 6685 (2024), <https://doi.org/10.1007/s10853-024-09577-6>
- <sup>24</sup> C. Felgueiras, N. G. Azoia, C. Gonçalves, M. Gama and F. Dourado, *Front. Bioeng. Biotechnol.*, **9**, (2021), <https://doi.org/10.3389/fbioe.2021.608826>
- <sup>25</sup> T. Y. D. Trang, H. T. Dzung, T. T. Huong and P. H. Quynh, *J. Phys. Conf. Ser.*, **2697**, 012049 (2024), <https://doi.org/10.1088/1742-6596/2697/1/012049>
- <sup>26</sup> E. A. Carter, B. Swarbrick, T. M. Harrison and L. Ronai, *Herit. Sci.*, **8**, 51 (2020), <https://doi.org/10.1186/s40494-020-00395-y>
- <sup>27</sup> M. Zaborowska, K. Bernat, B. Pyszczółkowski, D. Kulikowska and I. Wojnowska-Baryła, *Waste Manag.*, **168**, 413 (2023), <https://doi.org/10.1016/j.wasman.2023.06.022>
- <sup>28</sup> E. R. Kenawy, M. M. Azaam, M. Afzal, A. Khatoon, M. T. Ansari *et al.*, in "Tailor-Made Polysaccharides in Biomedical Applications", edited by A. Nayak, M. Saquib Hasnain and T. Aminabhavi, Academic Press, 2020, pp. 305-328, <https://doi.org/10.1016/B978-0-12-821344-5.00013-8>
- <sup>29</sup> S. Saedi, J. T. Kim, E. H. Lee, A. Kumar and G. H. Shin, *Ind. Crop. Prod.*, **197**, 116554 (2023), <https://doi.org/10.1016/j.indcrop.2023.116554>
- <sup>30</sup> N. A. Mohd Jamil, S. S. Jaffar, S. Saallah, M. Misson, S. Siddiquee *et al.*, *Nanomater. (Basel)*, **12**, 3537 (2022), <https://doi.org/10.3390/nano12193537>
- <sup>31</sup> K. Dhali, M. Ghasemlou, F. Daver, P. Cass and B. Adhikari, *Sci. Total. Environ.*, **775**, 145871 (2021), <https://doi.org/10.1016/j.scitotenv.2021.145871>

- <sup>32</sup> X. Yang, S. K. Biswas, J. Han, S. Tanpichai, M. C. Li *et al.*, *Adv. Mater.*, **33**, 2002264 (2021), <https://doi.org/10.1002/adma.202002264>
- <sup>33</sup> J. Xiao, H. Li, H. Zhang, S. He, Q. Zhang *et al.*, *J. Bioresour. Bioprod.*, **7**, 245 (2022), <https://doi.org/10.1016/j.jobab.2022.05.003>
- <sup>34</sup> Z. Niu, W. Cheng, M. Cao, D. Wang, Q. Wang *et al.*, *Nano Energ.*, **87**, 106175 (2021), <https://doi.org/10.1016/j.nanoen.2021.106175>
- <sup>35</sup> K. N. M. Amin, A. Hosseinmardi, D. J. Martin and P. K. Annamalai, *J. Bioresour. Bioprod.*, **7**, 99 (2022), <https://doi.org/10.1016/j.jobab.2021.12.002>
- <sup>36</sup> A. S. Hossain, M. U. Musamma, M. F. M. Fawzi and V. N. Veettil, *Adv. Biores.*, **7**, 5 (2016)
- <sup>37</sup> T. S. Franco, *Nov. Tech. Nutr. Food Sci.*, **1**, 2016 (2018), <https://doi.org/10.31031/NTNF.2018.01.000514>
- <sup>38</sup> M. Y. Leong, Y. L. Kong, M. Y. Harun, C. Y. Looi and W. F. Wong, *Carbohyd. Res.*, **532**, 108899 (2023), <https://doi.org/10.1016/j.carres.2023.108899>
- <sup>39</sup> C. H. Nguyen and D. Q. Le, *Iranian J. Chem. Chem. Eng.*, **42**, 27 (2023)
- <sup>40</sup> A. Septevani, D. Burhani and Y. Sampora, "Nanocellulose Materials", edited by R. Oraon, D. Rawtani, P. Singh and C. Mustansar Hussain, Elsevier, 2022, pp. 217-246, <https://doi.org/10.1016/B978-0-12-823963-6.00010-7>
- <sup>41</sup> G. Parikh, B. Parikh, A. Natu and D. Rawtani, "Nanocellulose Materials", edited by R. Oraon, D. Rawtani, P. Singh and C. Mustansar Hussain, Elsevier, 2022, pp. 157-178, <https://doi.org/10.1016/B978-0-12-823963-6.00009-0>
- <sup>42</sup> M. A. Aziz, M. Zubair and M. Saleem, *Case Studies Constr. Mater.*, **15**, e00761 (2021), <https://doi.org/10.1016/j.cscm.2021.e00761>
- <sup>43</sup> W. Hosakun, D. Tsalagkas and L. Csóka, *Innovation in Nano-Polysaccharides for Eco-Sustainability*, edited by P. Singh, K. Manzoor, S. Ikram, P. Kumar Annamalai, Elsevier, 2022, pp. 343-351, <https://doi.org/10.1016/B978-0-12-823439-6.00007-6>
- <sup>44</sup> R. E. Souza, F. J. B. Gomes and E. O. Brito, *J. Appl. Biotech. Bioeng.*, **7**, 100 (2020), <https://doi.org/10.15406/jabb.2020.07.00222>
- <sup>45</sup> S. Zhang, Z. Wang, Y. Zhang, H. Pan and L. Tao, *Proc. Environ. Sci.*, **31**, 3 (2016), <https://doi.org/10.1016/j.proenv.2016.02.001>
- <sup>46</sup> T. Wang, M. Jiang, X. Yu, N. Niu and L. Chen, *Separ. Purif. Technol.*, **302**, 122116 (2022), <https://doi.org/10.1016/j.seppur.2022.122116>
- <sup>47</sup> P. Penjumras, R. B. A. Rahman, R. A. Talib and K. Abdan, *Agric. Agric. Sci. Proc.*, **2**, 237 (2014), <https://doi.org/10.1016/j.aaspro.2014.11.034>
- <sup>48</sup> S. Wanlapa, K. Wachirasiri, D. Sithisam-ang and T. Suwannatup, *Int. J. Food Prop.*, **18**, 1306 (2011), <https://doi.org/10.1080/10942912.2010.535187>
- <sup>49</sup> X. Cui, J. Lee, K. R. Ng and W. N. Chen, *ACS Sustain. Chem. Eng.*, **9**, 1304 (2021), <https://doi.org/10.1021/acssuschemeng.0c07705>
- <sup>50</sup> A.-M. M. María, P. F. Maria, T.-B. D. Rita and M. Florencia, *Carbohyd. Polym.*, **123**, 406 (2015), <https://doi.org/10.1016/j.carbpol.2015.01.027>
- <sup>51</sup> L. Aguirre, L. Cámara and A. Smith, *Anim. Feed Sci. Technol.*, **293**, 115473 (2022), <https://doi.org/10.1016/j.anifeedsci.2022.115473>
- <sup>52</sup> J. Neue Kjedahl, *J. Anal. Chem.*, **22**, 366 (1883), <https://doi.org/10.1007/BF01338151>
- <sup>53</sup> K. Song, X. Zhu, W. Zhu and X. Li, *Bioresour. Bioprocess.*, **6**, 45 (2019), <https://doi.org/10.1186/s40643-019-0279-z>
- <sup>54</sup> X. An, Y. Wen, D. Cheng, X. Zhu and Y. Ni, *Cellulose*, **23**, 2409 (2016), <https://doi.org/10.1007/s10570-016-0964-4>
- <sup>55</sup> S. Liu, M. Zhang and D. Hong, *Enzyme Microb. Technol.*, **169**, 110289 (2023), <https://doi.org/10.1016/j.enzmictec.2023.110289>
- <sup>56</sup> L. Q. Dien and T. K. Anh, *J. Japan Inst. Energ.*, **100**, 135 (2021), <https://doi.org/10.3775/jie.100.135>
- <sup>57</sup> A. Atakhanov, I. Turdikulov, B. Mamadiyrov, N. Abdullaeva, I. Nurgaliev *et al.*, *Open J. Polym. Chem.*, **9**, 117 (2019), <https://doi.org/10.4236/ojpcchem.2019.94010>
- <sup>58</sup> Y. W. Chen, M. A. Hasanulbasori, P. F. Chiat and H. V. Lee, *Int. J. Biol. Macromol.*, **123**, 1305 (2019), <https://doi.org/10.1016/j.ijbiomac.2018.10.013>
- <sup>59</sup> S. R. Masrol, M. H. I. Ibrahim, S. Adnan, R. R. Abdul, A. M. Sa'adon, K. I. Sukarno and M. F. H. Yusoff, *J. of Tropical Forest Sci.*, **30**(1), 106–116, (2018), <http://doi.org/10.26525/jtfs2018.30.1.106116>
- <sup>60</sup> V. Raju, R. Revathiswaran, K. S. Subramanian, K. T. Parthiban, K. Chandrakumar *et al.*, *Sci. Rep.*, **13**, 1199 (2023), <https://doi.org/10.1038/s41598-022-26600-5>
- <sup>61</sup> C. Cara, E. Ruiz, I. Ballesteros, M. J. Negro and E. Castro, *Process Biochem.*, **41**, 423 (2006), <https://doi.org/10.1016/j.procbio.2005.07.007>
- <sup>62</sup> M. Kienberger, S. Maitz, T. Pichler and P. Demmelmayer, *Processes*, **9**, 804 (2021), <https://doi.org/10.3390/pr9050804>
- <sup>63</sup> N. A. N. Mohamad and J. Jai, *Heliyon*, **8**, e09114 (2022), <https://doi.org/10.1016/j.heliyon.2022.e09114>
- <sup>64</sup> G. T. Melesse, F. G. Hone and M. A. Mekonnen, *Adv. Mater. Sci. Eng.*, **2022**, 1 (2022), <https://doi.org/10.1155/2022/1712207>
- <sup>65</sup> S. S. Handayani, Amrullah, H. Fatimah and R. Seftiani, *J. Phys. Conf. Ser.*, **1280**, 022012 (2019), <https://doi.org/10.1088/1742-6596/1280/2/022012>
- <sup>66</sup> W. Han and Y. Geng, *Cellulose*, **30**, 4889 (2023), <https://doi.org/10.1007/s10570-023-05195-8>
- <sup>67</sup> C. I. Madueke, S. D. Pandita, F. Biddlestone and G. F. Fernando, *J. Indian Acad. Wood Sci.*, **21**, 100 (2024), <https://doi.org/10.1007/s13196-023-00328-9>
- <sup>68</sup> S. H. Osong, S. Norgren and P. Engstrand, *Cellulose*, **23**, 93 (2016), <https://doi.org/10.1007/s10570-015-0798-5>
- <sup>69</sup> R. D'Orsi, N. D. Fidio, C. Antonetti, A. M. R. Galletti and A. Operamolla, *ACS Sustain. Chem. Eng.*,

- 11**, 1875 (2023), <https://doi.org/10.1021/acssuschemeng.2c06356>
- <sup>70</sup> B. Yu, G. Fan and S. Zhao, *Appl. Biol. Chem.*, **64**, 15 (2021), <https://doi.org/10.1186/s13765-020-00579-x>
- <sup>71</sup> J. X. Sun, X. F. Sun, H. Zhao and R. C. Sun, *Polym. Degrad. Stabil.*, **84**, 331 (2004), <https://doi.org/10.1016/j.polymdegradstab.2004.02.008>
- <sup>72</sup> E. Korotkova, A. Pranovich, J. Wärnå, T. Salmi, D. Y. Murzin *et al.*, *Green Chem.*, **17**, 5058 (2015), <https://doi.org/10.1039/C5GC01341K>
- <sup>73</sup> E. Galiwango, N. S. Abdel Rahman, A. H. Al-Marzouqi, M. M. Abu-Omar, A. A. Khaleel, *Heliyon*, **5**, e02937 (2019), <https://doi.org/10.1016/j.heliyon.2019.e02937>
- <sup>74</sup> M. Szymańska-Chargot, M. Chylińska, K. Gdula, A. Koziół and A. Zdunek, *Polymers (Basel)*, **9**, 495 (2017), <https://doi.org/10.3390/polym9100495>
- <sup>75</sup> F. Reséndez-González, C. F. Castro-Guerrero, A. B. Morales-Cepeda, J. L. Rivera-Armenta and O. Solís-Canto, *Cellulose Chem. Technol.*, **58**, 323 (2024), <https://doi.org/10.35812/CelluloseChemTechnol.2024.58.31>
- <sup>76</sup> Z. Guomin, D. Jun, C. Weimin, P. Mingzhu and C. Dengyu, *Cellulose*, **26**, 8625 (2019), <https://doi.org/10.1007/s10570-019-02683-8>
- <sup>77</sup> B. Sitorus, I. Syahbanu, F. Yoni, Antonius and S. D. Panjaitan, *Cellulose Chem. Technol.*, **58**, 223 (2024), <https://doi.org/10.35812/CelluloseChemTechnol.2024.58.22>
- <sup>78</sup> Y. Ma, X. Chai, H. Bao, Y. Huang and W. Dong, *PLoS ONE*, **18**, e0281142 (2023), <https://doi.org/10.1371/journal.pone.0281142>
- <sup>79</sup> T. Rashid, C. F. Kait and T. Murugesan, *Procedia Eng.*, **148**, 1312 (2016), <https://doi.org/10.1016/j.proeng.2016.06.547>
- <sup>80</sup> Q. Zhang, H. Li, Z. Guo and F. Xu, *Polymers*, **12**, 378 (2020), <https://doi.org/10.3390/polym12020378>
- <sup>81</sup> O. Faix, *Holzforchung*, **45**, 21 (1991), <https://doi.org/10.1515/hfsg.1991.45.s1.21>
- <sup>82</sup> M. Saber, L. E. Hamdaoui, M. E. Moussaouiti and M. Tabyaoui, *Cellulose Chem. Technol.*, **56**, 69 (2022), <https://doi.org/10.35812/CelluloseChemTechnol.2022.56.06>
- <sup>83</sup> K. Shweta and H. Jha, *Biotech. Rep. (Amst)*, **7**, 95 (2015), <https://doi.org/10.1016/j.btre.2015.05.003>
- <sup>84</sup> M. Harahap, Y. A. Perangin-Angin, V. Purwandari, R. Goei, A. L. Y. Tok and S. Gea, *Heliyon*, **9**, e14556 (2023), <https://doi.org/10.1016/j.heliyon.2023.e14556>
- <sup>85</sup> Q. Hongyun, W. Jiake and Y. Lifeng, *J. Biores. Bioprod.*, **5**, 204 (2020), <https://doi.org/10.1016/j.jobab.2020.07.006>
- <sup>86</sup> A. L. M. P. Leite, C. D. Zanon and F. C. Menegalli, *Carbohydr. Polym.*, **157**, 962 (2017), <https://doi.org/10.1016/j.carbpol.2016.10.048>
- <sup>87</sup> L. D. Tolesa, S. G. Bhupender and L. Ming-Jer, *ACS Omega*, **3**, 10866 (2018), <https://doi.org/10.1021/acsomega.8b01447>
- <sup>88</sup> A. Zitting, A. Paajanen and P. A. Penttilä, *Cellulose*, **30**, 8107 (2023), <https://doi.org/10.1007/s10570-023-05357-8>
- <sup>89</sup> S. Haouache, C. Jimenez-Saelices and F. Cousin, *Cellulose*, **29**, 1567 (2022), <https://doi.org/10.1007/s10570-021-04313-8>
- <sup>90</sup> F. Stieler and B. Tonn, *Int. J. Metalcast.*, **18**, 1926 (2024), <https://doi.org/10.1007/s40962-023-01221-4>
- <sup>91</sup> A. Oun and J. W. Rhim, *Cellulose*, **25**, 2143 (2018), <https://doi.org/10.1007/s10570-018-1730-6>
- <sup>92</sup> D. Trache, A. F. Tarchoun, M. Derradji, T. S. Hamidon, N. Masruchin *et al.*, *Front. Chem.*, **8**, 32435633 (2020), <https://doi.org/10.3389/fchem.2020.00392>
- <sup>93</sup> M. T. Hossen, C. K. Kundu and B. R. R. Pranto, *Heliyon*, **10**, e25270 (2024), <https://doi.org/10.1016/j.heliyon.2024.e25270>
- <sup>94</sup> Y. Liu, B. Guo, Q. Xia, J. Meng, W. Chen *et al.*, *ACS Sustain. Chem. Eng.*, **5**, 7623 (2017), <https://doi.org/10.1021/acssuschemeng.7b00954>
- <sup>95</sup> N. N. An and P. T. Le Chi, *Vietnam J. Chem.*, **61**, 73 (2023), <https://doi.org/10.1002/vjch.202300070>
- <sup>96</sup> H. M. Shaikh, A. Anis, A. M. Poulouse, S. M. Al-Zahrani, N. A. Madhar *et al.*, *Molecules*, **27**, 1434 (2022), <https://doi.org/10.3390/molecules27041434>
- <sup>97</sup> D. N. Lam, D. V. H. Thien, C. N. Nguyen, N. T. T. Nguyen, N. Van Viet *et al.*, *Carbohydr. Polym.*, **297**, 120009 (2022), <https://doi.org/10.1016/j.carbpol.2022.120009>
- <sup>98</sup> M. Mariano, R. Cercena and V. Soldi, *Ind. Crop. Prod.*, **94**, 454 (2016), <https://doi.org/10.1016/j.indcrop.2016.09.011>
- <sup>99</sup> M. M. El-Sheekh, W. E. Yousuf, E. R. Kenawy and T. M. Mohamed, *Sci. Rep.*, **13**, 10188 (2023), <https://doi.org/10.1038/s41598-023-37287-7>
- <sup>100</sup> M. Poletto, *Maderas Sien. Tech.*, **19**, (2017), <http://dx.doi.org/10.4067/S0718-221X2017005000006>
- <sup>101</sup> Q. Yan, Ph.D. Thesis, Mississippi State University, Starkville, MS, USA, 2017, <https://scholarsjunction.msstate.edu/td/971>
- <sup>102</sup> Q. Yan, J. Li, X. Zhang, J. Zhang and Z. Cai, *Nanomaterials*, **8**, 840 (2018), <https://doi.org/10.3390/nano8100840>